Journal of Applied Polymer Science

Synthesis and Properties of Silver Nanoparticles in Chitosan-Based Thermosensitive Semi-Interpenetrating Hydrogels

Guiying Li, Quanwu Wen, Ting Zhang, Yuanyuan Ju
College of Chemistry and Materials Science, Ludong University, Yantai 264025, China
Correspondence to: G. Li (E-mail: guiyingli@126.com)

ABSTRACT: In this article, thermosensitive poly(*N*-isopropyl acrylamide-*co*-vinyl pyrrolidone)/chitosan [P(NIPAM-*co*-NVP)/CS] semi-interpenetrating (semi-IPN) hydrogels were prepared by redox-polymerization using *N*,*N*-methylenebisacrylamide as crosslinker and ammonium persulfate/*N*,*N*,*N*′,*N*′-tetramethylethylenediamine as initiator. Highly stable and uniformly distributed Ag nanoparticles were prepared by using the semihydrogel networks as templates via *in situ* reduction of silver nitrate in the presence of sodium borohydride as a reducing agent. Introduction of CS improves the hydrogels swelling ratio (SR) and stabilizes the formed Ag nanoparticles in networks. Scanning electron microscopy and transmission electron microscopy revealed that Ag nanoparticles were well dispersed with diameters of 10 nm. The semi-IPN hydrogel/Ag composites had higher SR and thermal stability than its corresponding semi-IPN hydrogels. © 2012 Wiley Periodicals, Inc. J. Appl. Polym. Sci. 000: 000–000, 2012

KEYWORDS: Ag nanoparticles; chitosan; composites; semi-interpenetrating hydrogels; sensitive hydrogels

Received 17 July 2011; accepted 24 February 2012; published online
DOI: 10.1002/app.37609

INTRODUCTION

In recent years, the synthesis and stabilization of metal nanoparticles has attracted great interest for their potential applications in catalysis, biochemistry, separation, electronic materials, and so on.[1–5] Generally, metal nanoparticles tend to agglomerate due to high active surface area. To stabilize the nanoparticles, various polymeric agents including polymeric micelles, dendrimers, latex particles, microgels, and hydrogels are used.[6–8] Among of these supports, hydrogels are extensively used *in situ* synthesis of smaller size metal nanoparticles due to their three-dimensional networks and good biocompatibility. The swollen hydrogels provide large free space between the crosslinked networks that can act as matrices or protecting agents against aggregation of nanoparticles a nanoreactor for nucleation and growth of nanoparticles.

Furthermore, size and morphology of the nanoparticles stabilized in hydrogels can be easily controlled by varying the amount of monomer, crosslinker, and functionality of hydrogel networks.[9,10]

Stimuli-sensitive hydrogels, which exhibit dramatic changes in their swelling behaviors and network structures in response to environmental stimuli, have been used to synthesize metal nanoparticles in recent years.[11–14] The combination of smart polymeric architectures with metal nanoparticles is a promising route to design novel materials with wide applications in biomedical field and catalytic systems.[15,16] Palladium nanoparticles embedded into hydrogels exhibit a high catalytic stability with higher selectivity for allyl alcohol hydrogenation and cyclohexane oxidation reactions.[15] When the catalyst of noble metal nanoparticles is immobilized within the thermosensitive hydrogels, it is expected to have a special advantage of easy separation and reuse through the reversible deswelling/swelling of the thermoresponsive hydrogel.[5,17]

Ag nanoparticles, which are nontoxic and environmentally friendly, demonstrate strong antimicrobial activity and excellent catalytic applications for a bridge between homogeneous and heterogeneous catalyses.[18–20] Although a number of hydrogel, microgel, and nanogel systems were utilized as templates to produce metal nanoparticles, there are few reports on Ag nanoparticles synthesized in thermosensitive semi-interpenetrating (semi-IPN) hydrogels.[21] Carbohydrates as renewable materials with hydrophilic nature for anchoring/reduction of metal ions and stabilization have attracted much attentions recently. Vimala et al. prepared silver nanoparticles in poly(acrylamide) semi-IPN hydrogels in presence gum acacia, carboxymethylcellulose and starch.[22] In this article, we synthesized thermosensitive poly(*N*-isopropyl acrylamide-*co*-vinyl pyrrolidone)/chitosan [P(NIPAM-*co*-NVP)/CS] semi-IPN hydrogels and studied its applications in controlled synthesis of Ag nanoparticles. PNIPAM is an excellent thermosensitive and

Table I. Feed Compositions of Hydrogels

Samples	CS (g)	NIPAM (g)	NVP (g)	MBA (g)	APS (g)	TMEDA (mL)
P(NIPAM-*co*-NVP)	0	4.52	1.50	0.082	0.075	0.15
Semi-IPN1	0.50	4.52	1.50	0.082	0.075	0.15
Semi-IPN2	1.00	4.52	1.50	0.082	0.075	0.15
Semi-IPN3	1.50	4.52	1.50	0.082	0.075	0.15
Semi-IPN4	1.50	4.52	1.50	0.105	0.075	0.15
Semi-IPN5	1.50	4.52	1.50	0.125	0.075	0.15
Semi-IPN6	1.50	4.52	1.50	0.06	0.075	0.15

biocompatible material. The combination of CS with PNIPAM creates novel intelligent hydrogels, which will be useful in the range of applications in electronics, biosensors, and drug delivery systems. Active —NH_2 and —OH groups in CS molecules may act as head groups to adsorb and stabilize Ag. In addition, introducing CS into polymer chains causes the hydrogels to be sensitive to pH so as to load Ag^+ at various swelling ratios (SR) to change the size and morphology of reduced Ag nanoparticles.[23]

EXPERIMENTAL

Materials

N-Isopropylacrylamide (NIPAM) (Acros Organics) was purified by recrystallization in benzene/*n*-hexane mixtures and dried in a vacuum. *N*-Vinyl pyrrolidone (NVP; National Medicine Group Chemical Reagent Company, China) was distilled under vacuum to eliminate the stabilizer before use. CS (Shanghai, China) with a deacetylation degree of 90% and viscosity-average molecular weight of 2.0×10^5 g/mol was purified by dissolving in aqueous acetic acid and precipitated by aqueous NaOH, then washed with water and ethanol and dried in a vacuum oven. Ammonium persulfate (APS), *N*,*N*,*N*′,*N*′-tetramethylethylenediamine (TMEDA), *N*,*N*-methylenebisacrylamide (MBA), silver nitrate ($AgNO_3$), and sodium borohydride ($NaBH_4$) were of analytical grade and used as received without further purification.

Synthesis of Semi-IPN Hydrogels

P(NIPAM-*co*-NVP)/CS semi-IPN hydrogels were synthesized by free radical polymerization using MBA as cross-linker and APS/TMEDA as redox-initiating pair. Briefly, NIPAM (4.52 g) and NVP (1.50 g) was first dissolved in 50-mL 4% dilute acetic acid (HAc) solution with different amounts of CS in a 150-mL three-necked round-bottom flask. Then, a given amounts of MBA (crosslinker), APS (initiator, 0.075 mg), and TMEDA (accelerator, 0.15 mL) were added under stirring. Polymerization was performed at 40°C for 24 h after degassed for 30 min. The hydrogel codes and feed composition were shown in Table I. After polymerization, the resulting hydrogels were sliced into small cylinders and then immersed in distilled water for 3 days by changing the water every 12 h to remove the residual monomers and other soluble agents. The resulting swollen hydrogels were dried in a vacuum oven at 40°C until to attain constant weight.

Preparation of Semi-IPN Hydrogel/Ag Composites

About 0.1-g dried semi-IPN hydrogel disks were equilibrated in distilled water for 3 days. The hydrogels were then transferred into a beaker containing 50 mL of $5 \times 10^{-3} M$ $AgNO_3$ aqueous solution, and then allowed to equilibrate for 1 day. During this stage, most of the Ag ions are transferred from the solution into hydrogel networks through the free-space between cross-linked networks or anchored to functional groups of polymeric chains. Then the Ag^+-loaded semi-IPN hydrogels were wiped with tissue paper and transferred to a beaker containing 50-mL $NaBH_4$ aqueous solution. The beaker was left in the refrigerator (4°C) for 2 h to reduce the Ag^+ into Ag nanoparticles and the hydrogel/Ag composites were separated.

Characterization

Fourier transform infrared spectroscopy (FTIR) was measured using Nicolet MAGNA550 FTIR spectrometer (UAS). The samples were dried completely, ground to fine power, and then pressed to disk mixed with KBr. Scanning was carried out in the wavelength region from 500 to 4000 cm^{-1} at ambient temperature.

The SR of hydrogels was studied in water by mass measurements after swollen to a desired time. Then, it was carefully taken out from the solution at given time intervals, wiped with a filter paper for the removal of the free water on the surface, and then weighted. The percentage of SR (g/g) was calculated as follows:

$$\mathrm{SR} = (w_t - w_d)/w_d$$

where w_d and w_t are the weights of dry and wet samples, respectively. The SR of hydrogel/Ag^+ and hydrogel/Ag composites was measured as similar as that of the hydrogel.

Scanning electron microscopy (SEM) morphology of semi-IPN hydrogels and hydrogel/Ag composites were sputtering-coated with a thin layer of palladium gold alloy and studied by using a JEOL JSM5610LV (Tokyo, Japan) SEM.

Transmission electron microscopy (TEM) image for hydrogel/Ag composites was recorded using a JEOL JEM-1230 TEM. For TEM measurements, finely ground hydrogel samples were dispersed in 1-mL distilled water. Then a drop of particle solution was placed on a copper grid and dried at room temperature after removing excess solution with filter paper.

The UV–vis absorption spectrum was recorded using a UV-2500 UV–vis spectrophotometer (Shimadzu, Japan) with a scan range of 200–600 nm.

X-Ray diffraction (XRD) measurements were performed for dried and finely grounded hydrogel samples on a Rigakud/

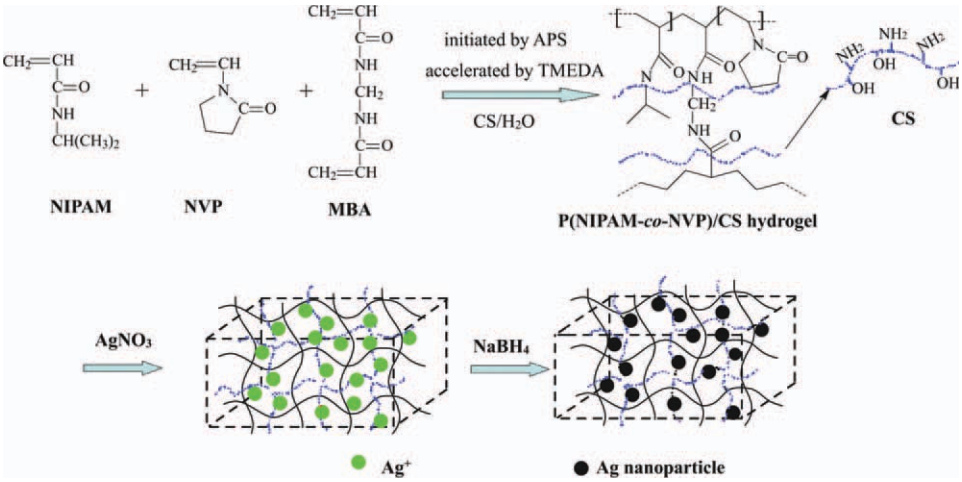

Figure 1. Synthesis of P(NIPAM-*co*-NVP)/CS semi-IPN hydrogels and hydrogel/Ag composites. [Color figure can be viewed in the online issue, which is available at wileyonlinelibrary.com.]

Max2500VPC diffractometer (Tokyo, Japan) with CuKα radiation ($\lambda = 0.1546$ nm) running at 40 kV and 200 mA. The average crystallite size (D) is calculated using Debye-Scherrer relationship:

$$D = k\lambda/\beta \cos \theta$$

where k is a constant of Scherrer ($k = 0.9$); λ is the wavelength of the incident X-ray; β is the full width at half maxima, and θ is the Bragg's diffraction angle.

The thermogravimetric analysis (TGA) of samples was evaluated using a Netzsch STA409 thermal system in a dynamic nitrogen atmosphere (flow rate 30 mL/min) at a heating rate of 10°C min^{-1}.

RESULTS AND DISCUSSION

Synthesis of Semi-IPN Hydrogel/Ag Composites

Because of the outstanding applications of hydrogel-metal nanoparticles in various fields, we designed a facile way to prepare Ag nanoparticles inside thermosensitive semi-IPN hydrogels. In this process, NIPAM and NVP were polymerized by free radical polymerization using MBA as crosslinker and APS/TMEDA as initiator in the presence of CS to obtain semi-IPN hydrogels. Figure 1 shows the synthesis procedure of P(NIPAM-*co*-NVP)/CS semi-IPN hydrogels and hydrogel/Ag composites.

Figure 2 shows the FTIR spectra of CS, P(NIPAM-*co*-NVP), and P(NIPAM-*co*-NVP)/CS semi-IPN hydrogels. Infrared spectrum of CS showed two strong peaks at 3420 and at 1630 cm^{-1} due to —OH stretching vibration and —NH bending vibration respectively. In Figure 2(b,c), the broad peak at 1660 cm^{-1} is the characteristic stretching of PNIPAM (amide I band, C=O stretching vibration mode conjugated with —NH groups on PNIPAM chains), which is conjugated with C=O stretching vibration of PVP network. The appearance of new peaks at 1540 and 1387 cm^{-1} are the —NH bending for secondary amides and isopropyl groups bending vibrations of PNIPAM, respectively. The peaks at 1290 and 1170 cm^{-1} are the characteristic stretching band for C—N and C=O of PVP. These values are in good agreement with that of reported in the literatures.[24]

P(NIPAM-*co*-NVP)/CS semi-IPN hydrogels are directly used as carriers for producing Ag nanoparticles. The immobilization of Ag nanoparticles throughout the hydrogel networks is due to the strong localization of Ag particles via bonding with functional groups of hydrogels. When semi-IPN hydrogels were equilibrated in $AgNO_3$ aqueous solutions, most of the Ag^+ were exchanged from solution into networks by the complexation with —NH_2, —OH, or —CONH groups of polymer chains. The reduction of various complexes with Ag^+ leads to the formation of Ag atoms, which is followed by agglomeration into oligomeric clusters.[25] The clusters eventually resulted in the formation of colloidal Ag nanoparticles. As shown in Figure 1, the nanoparticles were entrapped inside the networks through strong localization and stabilization established from the hydrogels. Formation of Ag nanoparticles in semi-IPN

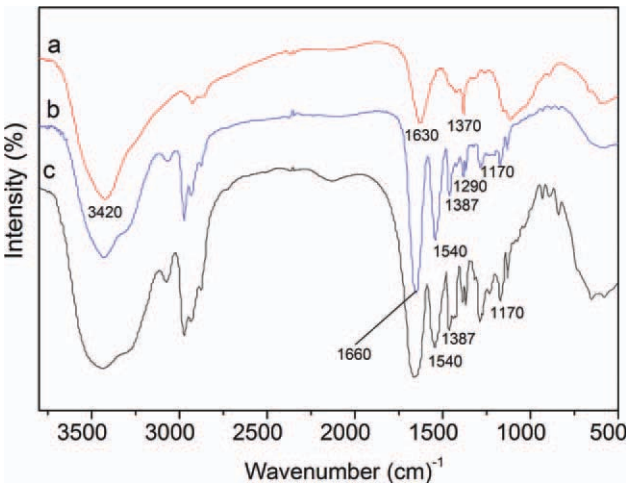

Figure 2. FTIR Spectra of (a) CS, (b) P(NIPAM-*co*-NVP), and (c) P(NIPAM-*co*-NVP)/CS semi-IPN hydrogel. [Color figure can be viewed in the online issue, which is available at wileyonlinelibrary.com.]

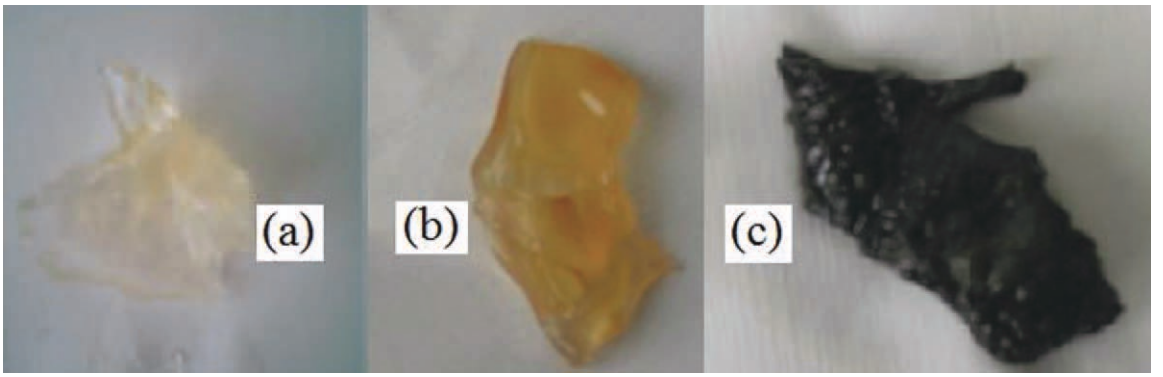

Figure 3. Photographs of (a) semi-IPN hydrogel, (b) Ag^+-loaded in hydrogel, and (c) hydrogel/Ag composites. [Color figure can be viewed in the online issue, which is available at wileyonlinelibrary.com.]

hydrogels can be expected because the Ag^+ loaded in networks were easily reduced by $NaBH_4$, which immediately turned into an opaque brown color as shown in Figure 3. This can be due to the adsorption of Ag nanoparticles through either nitrogen atoms or oxygen atoms present in the semi-IPN hydrogel macromolecular chains. In this way, highly distributed Ag nanoparticles were obtained within the semi-IPN hydrogel networks.

Swelling Property

The basic feature of hydrogel is that it can absorb and hold huge amount of water in its network structures. This property is very important as a carrier to load metal ions and to form metal nanoparticles from reduction reaction. Hence, we chosen natural polymers CS, which can also serve as stabilizers for Ag nanoparticles, to improve the swelling capacity of P(NIPAM-*co*-NVP) hydrogels at a given concentration of crosslinker. Figure 4 shows the swelling capacity of semi-IPN hydrogels, hydrogel-loaded Ag^+, and hydrogel/Ag composites. It was clear that the SR of semi-IPN hydrogels increased with the CS content. This is due to the fact that hydrophilic CS may create pore channels or porous surface morphology in the hydrogels network, which is convenient for the penetration of water into networks. On the other hand, both NIPAM and NVP are nonionic monomers which do not have ability for creating ionic interactions. While, CS is a cationic polysaccharide with water-binding capacity and has abundant hydration of functional groups (—OH and —NH_2) necessary for hydrogen interaction with water.[26,27] The amine groups of CS undergo ionization in aqueous solution and behave as cationic polyelectrolyte that causes increasing of swelling degree. Increasing the amount of CS within networks increases the more hydrophilicity of semi-IPN hydrogels; and more water molecules are absorbed within the networks. Therefore a higher swelling capacity for semi-IPN was obtained.

After precipitation of Ag nanoparticles within hydrogels, an increase in the SR was observed. From Figure 4, the order of swelling capacity was found as semi-IPN hydrogel/Ag^0 composite > semi-IPN hydrogel/Ag^+ > semi-IPN hydrogel. This is because the hydrogels treated with silver salt result in hydrogel networks with Ag^+ loaded throughout the network. The repulsion between Ag^+ with identical surface charges results in the expansion of the hydrogel network, which gives rise to an afflux of water to balance the build-up of ion osmotic pressure. The hydrogels containing Ag^+ treated with a reducing agent $NaBH_4$ yield Ag nanoparticles inside the networks, which, in turn, allows more water molecules to diffuse into the hydrogels. Similar swelling characteristics were achieved in many literatures.[22,28] The SR of semi-IPN hydrogels and hydrogel/Ag composite first increased and then decreased with the increase of MBA content. This could be explained by the fact that increasing MBA

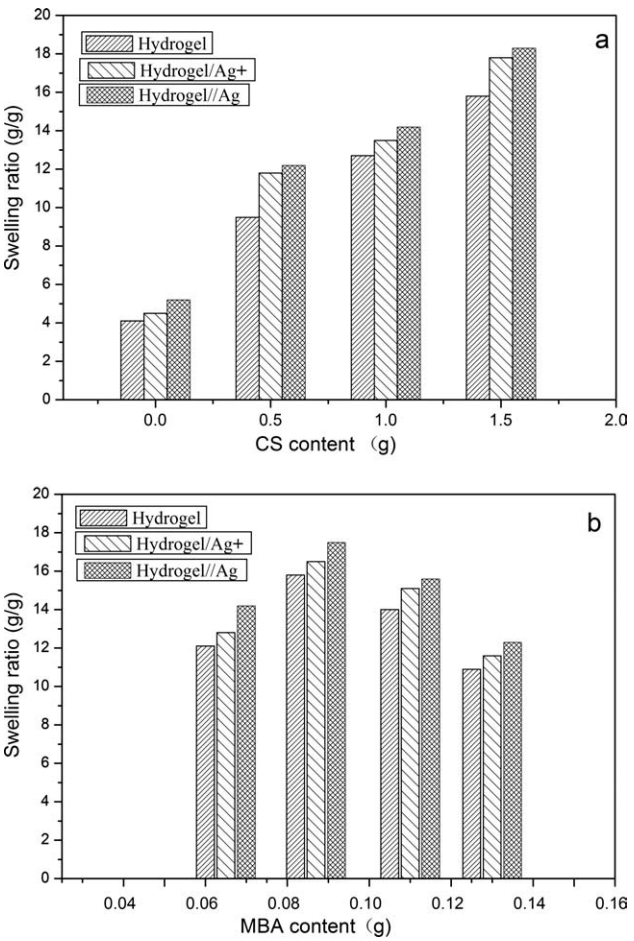

Figure 4. Effect of (a) CS and (b) MBA on the swelling ratio of semihydrogels, hydrogel/Ag^+, and hydrogel/Ag composite.

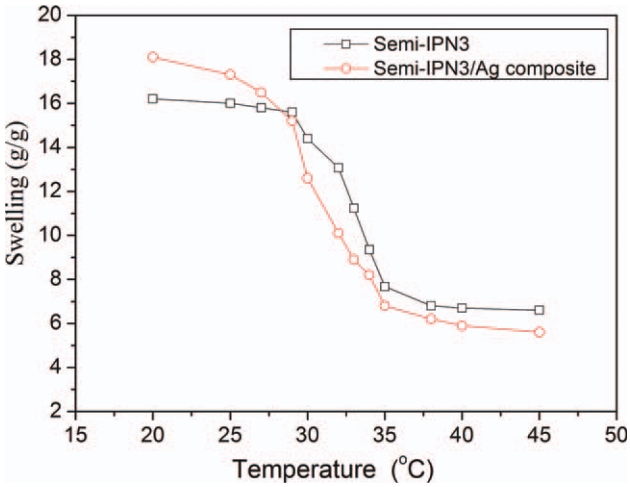

Figure 5. Effect of temperatures on the swelling ratio of semi-IPN hydrogels and hydrogel/Ag composites. [Color figure can be viewed in the online issue, which is available at wileyonlinelibrary.com.]

concentration at lower crosslinking density lead to the formation of hydrogel networks, which in favors of reserving water in hydrogels. Once the hydrogel network formed, further increasing MBA produces an additional network and decreases the mesh size of hydrogel. As a result, the water absorption reduced.

The dependence of SR as a function of temperatures was illustrated in Figure 5. As expected, P(NIPAM-*co*-NVP)/CS semi-IPN hydrogels and hydrogel/Ag composite were thermoresponsive as similar as general PNIPAM hydrogels. The SR of all samples was high at low temperature and decreased quickly when the temperature increased above the volume–phase transition temperature, where the phase separation of PNIPAM took place resulting from the breakdown of hydrogen bonds and the enhancement of hydrophobic interactions. Based on the SR experiments, the phase transition temperature is regarded as the temperature point at which the SR decreased dramatically. From Figure 5, semi-IPN hydrogels showed a temperature of phase transition at about 33.5°C. The phase transition temperature of the hydrogel/Ag composite is a little lower than that of corresponding semihydrogels, which is possibly due to the relatively strong interactions between encapsulated Ag nanoparticles and hydrogels.[5]

Microscopic Study of Composites

SEM images of pure hydrogels and hydrogel/Ag composites were shown in Figure 6. From Figure 6(a), it was clearly that

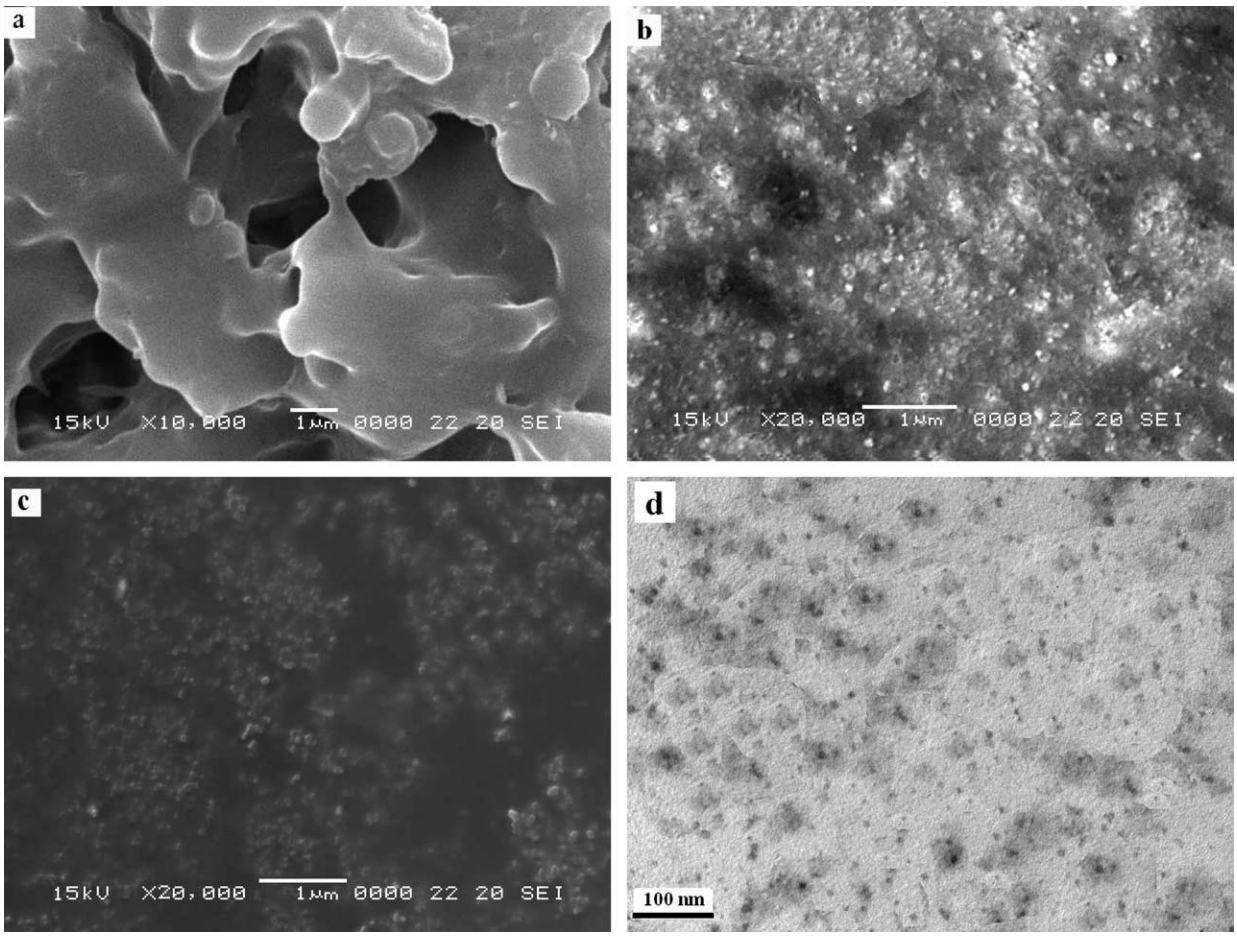

Figure 6. SEM images of (a) semi-IPN3 hydrogel, (b) Ag nanoparticles on the surface of hydrogel, (c) Ag nanoparticles inside the hydrogel (cross section), and (d) TEM image of Ag nanoparticles obtained from semi-IPN3 hydrogel.

Applied Polymer SCIENCE

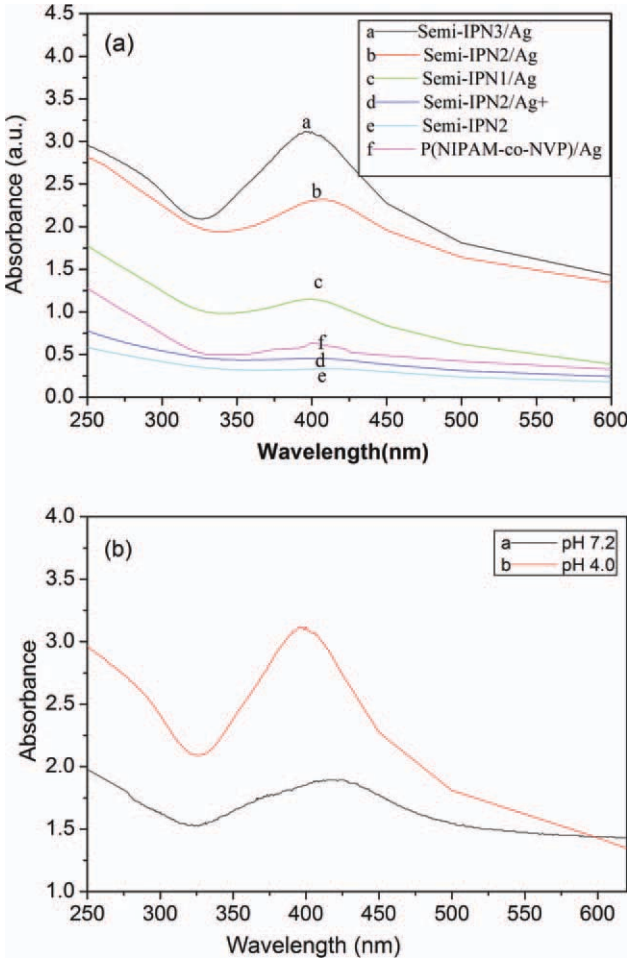

Figure 7. UV–vis spectra of (a) different hydrogel/Ag composites and (b) semi-IPN3 hydrogel/Ag composites loaded at different pH. [Color figure can be viewed in the online issue, which is available at wileyonlinelibrary.com.]

semi-IPN hydrogel has a porous structure, which is useful to increase accessibility for solution storing and encapsulating metal nanoparticles. Figure 6(b,c) illustrates the formation of Ag nanoparticles throughout the hydrogel networks. It was seen that Ag nanoparticles not only formed on the surfaces of semi-IPN hydrogels but also uniformly distributed inside the hydrogel networks. The presence of Ag nanoparticles inside the hydrogel networks may be attributed to Ag nanoparticles on the surface increase the hydrogel porosity, which provides a pathway for reducing agent to enter into the bulk inside hydrogel networks. The TEM image also indicates a highly uniform distribution of Ag nanoparticles inside hydrogel. It was confirmed that Ag nanoparticles formed in the crosslinked hydrogel networks are spherical, highly dispersed with diameters of about 10 nm.

UV–Vis Spectra Study of Composites

The presence of embedded Ag nanoparticles within hydrogel networks was confirmed by using UV–vis spectrophotometry. As presented in Figure 7(a), no absorption was found both in

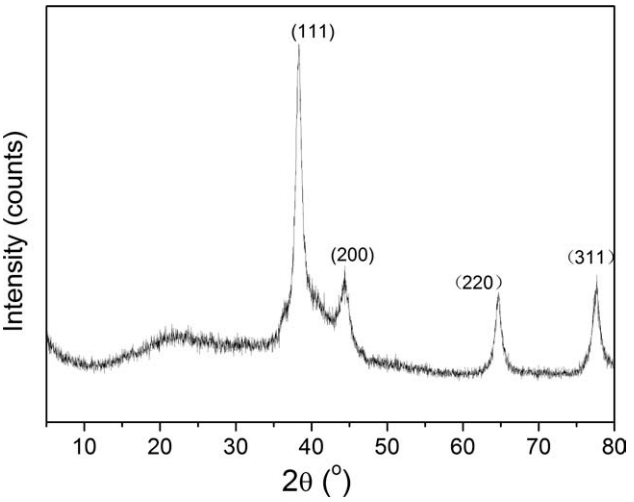

Figure 8. XRD patterns of semi-IPN3 hydrogel/Ag composite.

the case of blank hydrogel and hydrogel/Ag^+; whereas a distinct characteristic absorption peak at about 410 nm was observed for all hydrogel/Ag composites. The appearance of the absorption peak is due to the characteristic surface plasmon resonance effect of quantum-size Ag nanoparticles, which indicates that the colloidal Ag nanoparticles formed within the hydrogel networks.[29] A significant increase in absorption peak intensity was observed with the increase of CS content in hydrogels, indicating CS plays an excellent property for anchoring and stabilizing large amounts of Ag nanoparticles. Ag salt-loading capacity increases with the increase of CS, which results from the CS providing enough space to entrap more nanoparticles in networks. Meanwhile, linear polymer chains of CS promoted the stabilization of particles via bonding with —NH_2, —OH, —CONH, etc., functional groups. The more Ag nanoparticles formation within the net structure, in turn, positively increases the absorption in the UV–vis spectra. In all UV–vis spectra of hydrogel/Ag composites, there are no peaks identified around

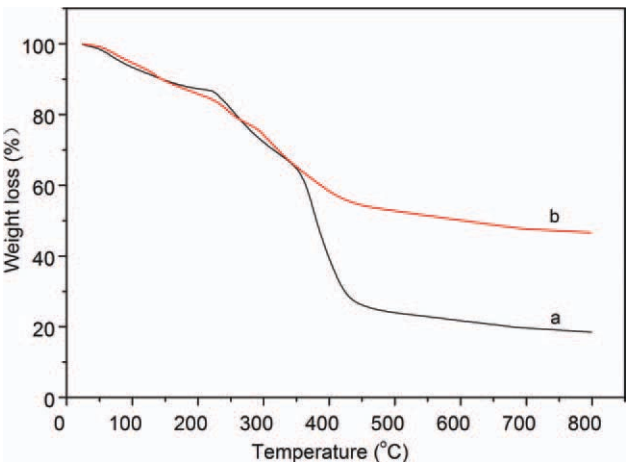

Figure 9. Thermograms of (a) semi-IPN3 hydrogel and (b) hydrogel/Ag composite. [Color figure can be viewed in the online issue, which is available at wileyonlinelibrary.com.]

335 and 560 nm, indicating the complete absence of Ag nanoparticle aggregation or Ag_n clusters.[7] This result proves that highly stable and well-dispersed Ag nanoparticles were successfully formed within the hydrogels. Compared to P(NIPAM-*co*-NVP)/CS semi-IPN hydrogel/Ag composites, the UV–vis spectrum absorption peak of P(NIPAM-*co*-NVP)/Ag composites was very lower.

Figure 7(b) shows the UV–vis spectra of semi-IPN hydrogel/Ag nanoparticle loaded at different pH. It was seen that the UV–vis spectra exhibit some differences due to that Ag^+ ions were loaded at different pH. In the curve of sample prepared at pH 4.0, a peak is observed at around 410 nm. A shoulder shifted to higher wavelengths (425 nm) and a decreased absorption was seen for Ag nanocomposite loaded at pH 7.2. This was attributed to particle formation by aggregating and growing in hydrogels with loaded SR of Ag^+ decreasing with pH.[14] This result indicates that the different loading conditions of Ag^+ ions before reduction have important effect on the morphology of reduced Ag nanoparticles.

XRD Study of Composites

The formation of Ag nanoparticles in semi-IPN hydrogels was further verified using XRD. As shown in Figure 8, the observed diffraction peaks of semi-IPN hydrogel/Ag composites at 38.1°, 44.3°, 64.5°, and 77.4° were assigned to (111), (200), (220), and (311) planes of the face-centered cubic of Ag nanoparticles, respectively.[22] This confirms the presence of Ag nanoparticles in the hydrogel networks. However, no such peaks were found in P(NIPAM-*co*-NVP)/CS semi-IPN hydrogels or hydrogels loaded with Ag salts. The average sizes of the Ag particles produced in semi-IPN hydrogels are estimated to be 12.1 nm according to the Debye-Scherrer equation.[30] It is observed that the crystallite size of the particles is consistent with that of measured from TEM.

TGA Study of Composites

The presence of Ag nanoparticles typically enhances the thermal stability of a hydrogel. As shown in Figure 9, semi-IPN hydrogel followed two degradation steps and exhibited 80 wt % weight losses below 450°C due to the degradation of polymer chains. However, in case of hydrogel/Ag composite, only 50 wt % weight loss below 500°C. Thus, TGA experiments demonstrated that hydrogel/Ag composite exhibited higher thermal stability compared to semi-IPN hydrogels. The weight loss difference between semi-IPN hydrogel and hydrogel/Ag composite indicates the presence of Ag nanoparticles in hydrogels.

CONCLUSIONS

In summary, controlled Ag nanoparticles were synthesized inside the P(NIPAM-*co*-NVP)/CS semi-IPN hydrogel networks. Introduction of CS into hydrogels plays an excellent property for anchoring and stabilization of Ag nanoparticles. The Ag nanoparticles immobilized throughout the hydrogel networks, not only on the surface but also inside the networks, was due to the complexation of Ag^+ with functional groups in polymer chains. Compared to pure semi-IPN hydrogels, the hydrogel/Ag composites displayed enhanced properties of equilibrium swelling and thermal stability. The fabrication of such hydrogel/Ag composites represents a promising route for creating complex particles in biomedical field and catalytic systems.

ACKNOWLEDGMENTS

The authors gratefully acknowledge the financial support by the National Natural Science Foundation of China (21074050), Natural Science Foundation of Shandong Province (ZR2011BQ007).

REFERENCES

1. Tokuyama, H.; Kanehara, A. *React. Funct. Polym.* **2007,** *67*, 136.
2. Wang, Z.; Tan, B.; Hussain, I.; Schaeffer, N.; Wyatt, M. F.; Brust, M.; Cooper, A. I. *Langmuir* **2007,** *23*, 885.
3. Saravanan, P.; Raju, M. P.; Alam, S. *Mater. Chem. Phys.* **2007,** *103*, 278.
4. Lu, Y.; Spyra, P.; Mei, Y.; Ballauff, M.; Pich, A. *Macromol. Chem. Phys.* **2007,** *208*, 254.
5. Wang, Y.; Yan, R.; Zhang, J.; Zhang, W. *J. Mol. Catal. A: Chem.* **2010,** *317*, 81.
6. Zhang, Y.; Liu, H.; Zhao, Y.; Fang, Y. *J. Colloid Interface Sci.* **2008,** *325*, 391.
7. Murthy, P. S. K.; Mohan, Y. M.; Varaprasada, K.; Sreedhar, B.; Raju, K. M. *J. Colloid Interface Sci.* **2008,** *318*, 217.
8. Madani, A.; Nessark, B.; Brayner, R.; Elaissari, H.; Jouini, M.; Mangeney, C.; Chehimi, M. M. *Polymer* **2010,** *51*, 2825.
9. Luo, Y. L.; Wei, Q. B.; Xu, F.; Chen, Y.-S.; Fan, L-H.; Zhang, C.-H. *Mater. Chem. Phys.* **2009,** *118*, 329.
10. Park, S.; Murthy, P. S. K.; Park, S.; Mohan, Y. M. Koh, W.-G. *J. Ind. Eng. Chem.* **2011,** *17*, 293.
11. Bikram, M.; Gobin, A. M.; Whitmire, R. E.; West, J. L. *J. Controlled Release* **2007,** *123*, 219.
12. Stavrouli, N.; Katsampas, I.; Aggelopoulos, S. Tsitsilians, C. *Macromol. Rapid Commun.* **2008,** *29*, 130.
13. Dayananda, K.; He, C.. Park, D. K.; Park, T. G.; Lee, D. S. *Polymer* **2008,** *49*, 4968.
14. Xiang, Y.; Chen, D. *Eur. Polym. J.* **2007,** *43*, 4178.
15. Kudaibergenov, S. E.; Ibraeva, Z. E.; Dolya, N. A.; Musabaeva, B. Kh.; Zharmagambetova, A. K.; Koetz, J. *Macromol. Symp.* **2008,** *274*, 1, 11.
16. Smith, J. R.; Capacio, B. R. NATO Science for Peace and Security Series-A: Chemistry and Biology. Springer Science+Business Media B.V., Netherlands, **2011;** Chapter 19, p. 181.
17. Wang, Y.; Zhang, J.; Zhang, W.; Zhang, M. *J. Org. Chem.* **2009,** *74*, 1923.
18. Xie, L.; Chen, M.; Wu, L. *J. Polym. Sci. Polym. Chem.* **2009,** *47*, 4919.
19. Gils, P. S.; Ray, D.; Sahoo, P. K. *Int. J. Biol. Macromol.* **2010,** *46*, 237.
20. Mohan, Y. M.; Lee, K.; Premkumar, T.; Geckeler, K. E. *Polymer* **2007,** *48*, 158.

21. Bajpai, S. K.; Mohan, Y. M.; Bajpai, M.; Thomas, V.; Namdeo, M. *J. Macromol. Sci. Pure Appl. Chem.* **2008,** *45*, 1.
22. Vimala, K.; Sivudu, K. S.; Mohan, Y. M.; Sreedhar, B.; Raju, K. M. *Carbohydr. Polym.* **2009,** *75*, 463.
23. Vimala, K.; Mohan, Y. M.; Sivudu, K. S.; Varaprasad, K.; Ravindra, S.; Reddy, N. N.; Padma, Y.; Sreedhar, B.; Mohana Raju, K. *Colloids Surf. B: Biointerf.* **2010,** *76*, 248.
24. Geever, L. M.; Cooney, C. C.; Lyons, J. G.; Kennedy, J. E.; Nugent, M. J. D.; Devery, S.; Higginbotham, C. L. *Eur. J. Pharm. Biopharm.* **2008,** *69*, 1147.
25. Babu, V. R.; Kim, C.; Kim, S.; Ahn, C.; Lee, Y.-I. *Carbohydr. Polym.* **2010,** *81*, 196.
26. Kim, I.-Y.; Yoo, M.-K.; Kim, B.-C.; Kim, S.-K.; Lee, H.-C.; Cho, C.-S. *Int. J. Biol. Macromol.* **2006,** *38*, 51.
27. Verestiuc, L.; Ivanov, C.; Barbu, E.; Tsibouklis, J. *Int. J. Pharm.* **2004,** *269*, 185.
28. Mohan, Y. M.; Vimala, K.; Thomas, V.; Varaprasad, K.; Sreedhar, B.; Bajpai, S. K.; Raju, K. M. *J. Colloid Interface Sci.* **2010,** *342*, 73.
29. Thomas, V.; Yallapu, M. M.; Sreedhar, B.; Bajpai, S. K. *J. Colloid Interface Sci.* **2007,** *315*, 389.
30. Li, X. H.; Li, Y. C.; Tan, Y. W.; Yang, C. H.; Li, Y. F. *J. Phys. Chem. B* **2004,** *108*, 5192.